Macromolecules
ARTICLE

Macromolecules **XXXX**, *XXX*, 000–000 **A**
DOI: 10.1021/ma101695y

Distribution of Segmental Mobility in Ultrathin Polymer Films

Cinzia Rotella,[†] Simone Napolitano,*[,†] Lieven De Cremer,[‡] Guy Koeckelberghs,[‡] and Michael Wübbenhorst[†]

[†]*Katholieke Universiteit Leuven, Laboratory of Acoustic and Thermal Physics, Department of Physics and Astronomy, Celestijnenlaan 200D, B-3001 Leuven, Belgium, and* [‡]*Katholieke Universiteit Leuven, Laboratory of Molecular Electronics and Photonics, Department of Chemistry, Celestijnenlaan 200F, B-3001 Leuven, Belgium*

Received July 27, 2010

ABSTRACT: We investigated by dielectric relaxation spectroscopy the distribution of glass transition temperatures and dielectric relaxation strength inside ultrathin polymer films capped between metallic layers. Measurements of the local dielectric properties were achieved by selectively placing layers of dye-labeled polystyrene at different depth inside films of neat polystyrene of different thickness. We show experimental evidence for an interfacial nature of the deviations from bulk behavior; in particular, the value of the dielectric strength and the glass transition temperature strongly depend on the distance from the solid interface. These peculiar profiles of static and dynamic dielectric properties are discussed in terms of a physical picture based on competition between chain adsorption and packing frustration at different annealing conditions. Such a picture was able to rationalize common features observed in properties of ultrathin films like reduction of the relaxation strength, broadening of the dynamic glass transition process, and finally a shift of the structural relaxation time.

1. Introduction

The physical properties of polymers in the proximity of surfaces and interfaces have been widely investigated in the past years. The interest for polymer surfaces and ultrathin films arises from the development of nanofabrication processes, where the knowledge about the structure and dynamics of interfacial layers has significant implications.[1] Numerous experimental works have established that properties of confined polymers such as viscoelasticity,[2,3] crystallization kinetics,[4−7] diffusion,[8,9] and glass transition temperature (T_g)[10−12] display significant deviations from their bulk values. Substantial evidence supports the idea that the origin of those deviations is mainly related to interfacial interactions rather than to solely size effects. It was shown, for instance, that the presence of a free surface typically results in enhanced mobility of the chain segments near the surface, which effectively yields a surface layer with a reduced T_g, extending over a few nanometers inside the film.[3,13,14] The global mobility in ultrathin polymer films can also be affected by the presence of solid surfaces like for supported films (having both a free surface and an interface with a solid substrate) or capped films (layers embedded between two solid surfaces). Increases in T_g upon thickness reduction are commonly reported for polymers showing a strong chemical affinity with the substrate.[15,16] In this case, chain segments in proximity of the interface are adsorbed and their mobility is seriously hindered, leading to an increase of T_g.[17−19] In contrast, small variations of T_g are observed in case of weak or slightly repulsive interactions between the polymer and the substrate.[16] It is generally assumed that interfacial properties are directly governed by the strength of intermolecular interactions. Nevertheless, even in case of favorable polymer/substrate interactions, a reduction in T_g has been noticed and explained in terms of packing frustration of chain segments adsorbed at the solid interfaces.[20]

Hence, it is reasonable to assume that the interplay between chain adsorption and packing frustration gives rise to a profile of mobility and thus to a distribution of glass transition temperatures across the film thickness.[21−25] Despite substantial efforts to study the effect of interfaces on the polymer dynamics, it remains unclear how these perturbations propagate inside the film. A successful approach to achieve depth resolution for the glass transition temperature in ultrathin polymer films was proposed and exploited by Torkelson and co-workers using fluorescence techniques.[19,26−28] By placing a (fluorescent) dye-labeled polymer layer at a specific position within a stack of unlabeled polymer layers, it was possible to determine a volumetric glass transition temperature averaged over a depth region of typically 15 nm.[26]

In our experiment, we adopted the multilayer approach by taking advantage of the sensitivity of dielectric spectroscopy to determine the profile of the structural relaxation time-resolved along the thickness. In fact, this technique, in contrast to dilatometric measurements, is able to investigate the relaxation processes and thus the relaxation time distribution over a broad frequency range for temperatures extending from above to below the bulk glass transition. In addition to the information achieved on a depth profile of T_g, the investigation of the structural relaxation allowed us to map the molecular mobility also by means of the dielectric strength, a quantity proportional to the amount of *mobile* molecules relaxing on the time scale and the length scale of the dynamic glass transition.

The determination of the actual mobility depth profile via the multilayer approach is of crucial importance to test theoretical models and predictions of materials performances at the nanoscale, but it is also challenging from the experimental point of view. The study required the synthesis of a labeled polymer with specific properties such as a sufficient content of dye molecules that ensured an enhanced dielectric strength relative to the neat polymer and a high molecular weight in order to reduce the interdiffusion depth between consecutive layers.

In this study, we first describe the synthesis and the dielectric properties of high molecular weight (M_w) dye-labeled polystyrene (chromophore: disperse red one, DR1). Subsequently, we focus on the dynamics of bi- and trilayers of labeled PS (*l*-PS) and neat

*To whom correspondence should be addressed. E-mail: simone.napolitano@fys.kuleuven.be.

PS of similar M_w, discussing the impact of layer thickness and annealing conditions at different depth positions. Finally, we study the effect of annealing on the evolution of the profile of molecular mobility providing a solid physical picture of the changes of T_g in proximity of an interface.

2. Experimental Section

2.1. Synthesis of the Chromophore-Functionalized Polymer. Styrene (5.97 mL, 51.9 mmol), 3-(ethynyl)benzoic acid (222 mg, 1.50 mmol), and benzoyl peroxide (BPO) (2.1 mg) were mixed, purged with argon, and then stirred for 3 days at 70 °C. The polymer was dissolved in chloroform (100 mL) and precipitated in methanol and dried. This procedure was repeated twice. Oxalyl chloride (3.00 mL) was added to an argon-purged solution of the product (1.04 g) in dry toluene (200 mL). The mixture was stirred at 40 °C, and the reaction was followed with infrared spectroscopy. After completeness of the reaction (typically 5 h), the excess of oxalyl chloride was removed at reduced pressure. The chromophore was synthesized according to literature procedures.[29] To a solution of the polymer, bearing the acid chloride functionalities, in toluene was added 4-(dimethylamino)pyridine (DMAP) (855 mg, 7.00 mmol) and chromophore (2.59 g, 7.00 mmol), and the mixture was stirred overnight at 40 °C. After concentrating, the labeled polymer was precipitated in methanol and rinsed with methanol. The polymer was dissolved in toluene and successively precipitated in methanol, rinsed with methanol, and dried. This procedure was repeated three times.

Gel permeation chromatography (GPC) measurements were done with a Shimadzu 10A apparatus with a tunable absorbance detector and a differential refractometer in tetrahydrofuran (THF) as eluent toward polystyrene standards. The labeled PS used in this study had $M_n = 619\ \mathrm{kg\,mol^{-1}}$ and $M_w = 819\ \mathrm{kg\,mol^{-1}}$. The structure of the precursor polymers and the chromophore-functionalized PS was verified by ^{1}H nuclear magnetic resonance (NMR) measurements and were carried out with a Bruker Avance 300 MHz. The content of chromophore in the labeled PS (1.25%) was measured with UV−vis spectroscopy using a Varian Cary 400 apparatus. Atactic polystyrene (M_w = 932 kg/mol) was used as received from Polymer Source Inc. The glass transition temperature of both polymers (T_g^{DSC}(PS) = 105 ± 3 °C, T_g^{DSC}(*l*-PS) = 108 ± 3 °C) was measured by differential scanning calorimetric with an heating rate of 20 °C/min.

2.2. Preparation of Ultrathin Polymer Films and Multilayers. Ultrathin single layers of labeled PS (*l*-PS) and neat PS were prepared by spin-coating filtered solutions of the polymer in chloroform on glass slides, onto which a 50 nm thick layer of aluminum was previously deposited by thermal evaporation in a high vacuum ($p \leq 10^{-6}$ mbar). Films of different thickness were obtained by changing the concentration of the polymer in the solution. After deposition, all samples were annealed at 120 °C for 2 h on a hot plate in order to remove residual solvent and to reduce the mechanical stresses induced by the spin-coating procedure.[30] Subsequently, the samples were kept under high vacuum ($p \leq 10^{-6}$ mbar) for 1 h at room temperature. On completion, a second layer of patterned aluminum electrodes was evaporated on top of the polymer film, resulting in individual capacitors with an area of 4 mm^2. A fast evaporation rate (∼10 nm/s) was used to obtain sharp polymer/metal interfaces. Bilayer and trilayer films were prepared by spin-coating individual layers on mica sheets and subsequently floating them from a water reservoir onto the blank substrate or onto a previously deposited and annealed polymer layer. Water occasionally trapped between consecutive layers was allowed to evaporate at ambient conditions for a couple of days before the deposition of the next layer. After assembling, the multilayer films were further annealed at 110 °C for 1 h. Sample capacitors were obtained following the same procedure used for the single layer films. The annealing conditions and the high molecular weights used in this work permitted to obtain continuous films with labeled chains present only at particular depth within the film, in particular interdiffusion between neighboring layers was limited at 3 nm in the first heating run and reached 10 nm during the subsequent cooling rate.[31]

2.3. Dielectric Relaxation Spectroscopy. Dielectric measurements were recorded in the frequency range from 10^{-1} to 10^6 Hz using a high-resolution dielectric analyzer (Alpha Analyzer, Novocontrol Technologies). All measurements were performed under N_2 in a closed cell to prevent any possible oxidation or degradation. The thickness h of the samples was evaluated from the value of the capacitance at room temperature using the relation for the electrical capacitance in the geometry of parallel plates, $C' = \varepsilon'\varepsilon_0(S/h)$, where ε_0 is the permittivity of the vacuum, ε' is the permittivity of the polymer, and S is the effective area of the capacitor (4 mm^2).

For a quantitative analysis of the dielectric spectra in the frequency domain the α-peak was fitted with the empirical Havriliak−Negami (HN) function:

$$\varepsilon'' = -\mathrm{Im}\left\{\frac{\Delta\varepsilon}{(1+(i\omega\tau_{HN})^a)^b}\right\} + \frac{\sigma}{\varepsilon_0\omega} \quad (1)$$

where τ_{HN} is the mean relaxation time, $\Delta\varepsilon$ is the relaxation strength, and a and b shape parameters which describe the symmetric and asymmetric broadening of the α-peak, while the last term accounts for ohmic conduction. For a more detailed description of the fit procedure see ref 32. The dielectric strength $\Delta\varepsilon$, proportional to both the mean-square dipole moment and the density of dipoles, provides a measure of the amount of mobile chains involved in the structural relaxation.

The structural relaxation times τ_α, calculated from τ_{HN}, a, and b,[33] were fitted in terms of the empirical Vogel−Fulcher−Tammann equation (VFT), which describes the temperature dependence of supercooled liquid in the temperature range between T_g and the melting point, T_m:

$$\tau_\alpha = \tau_\infty \exp\left[\frac{E_V}{R(T-T_V)}\right] \quad (2)$$

Here, E_V is the activation energy in the high-temperature limit, T_V is the Vogel temperature, and τ_∞ denotes the ultimate relaxation time at $T \to \infty$.[34] From the VFT parameters we can evaluate an operationally defined glass transition temperature using the criterion $T_g = T(\tau_\alpha = 100\ \mathrm{s})$.

Multilayer films were modeled as a series of capacitance where C^*_{tot} is given by

$$\frac{1}{C^*_{tot}} = \frac{1}{C^*_{\text{labeled PS}}} + \frac{1}{C^*_{\text{neat PS}}}$$

$C^*_{\text{labeled PS}}$ and $C^*_{\text{neat PS}}$ are the complex capacitance relative to the *l*-PS and to the neat PS, respectively. From the knowledge of the intrinsic contribution of neat PS, it was possible to extract the contribution of the labeled layer from the total response of the multilayer film.

3. Results and Discussion

3.1. Effect of Confinement on the Dynamics of Single Layers of Neat and Labeled PS. Polystyrene has a low intrinsic dielectric activity due to the presence of a weakly polar C-phenyl side group that gives rise to the dielectric α-relaxation. This dielectric activity, expressed by the dielectric strength $\Delta\varepsilon$, however, can be facilitated by the addition of a small amount of dipolar molecules.[35] The idea of enhancing the dielectric response of a nearly apolar polymer by doping with molecular dipoles that are either dispersed (probes) or covalently attached to the polymer chain (labels) was recently extended to ultrathin polymer films.[36,37] For example, dispersion of 1% (w/w) of 4,4′-(*N*,*N*-dibutylamino)-(*E*)-nitrostilbene (DBANS) increases the dielectric strength of PS by a factor of 5,[35,38] while the dielectric loss

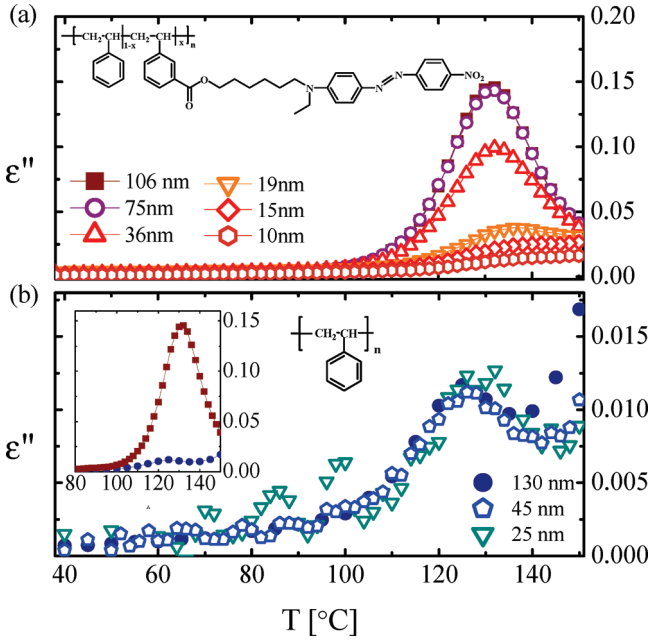

Figure 1. Temperature dependence of the imaginary part of the complex dielectric function ε'' (frequency f = 1 kHz, cooling) for films of (a) labeled PS and (b) neat PS of different thickness. The inset in (b) shows the comparison between ε'' (f = 1 kHz, cooling) for thick samples of labeled PS (h = 106 nm) and neat PS (h = 130 nm). Schemes of the repeating units are given.

of PS (M_w = 13 kg/mol) was shown to be enhanced 65 times after covalently attaching DR1 (3% w/w) directly onto the backbone.[37]

The inset in Figure 1 displays the imaginary component of the complex dielectric function, $\varepsilon''(T)$, measured upon cooling at 1 kHz for bulk samples of neat PS and *l*-PS of comparable thickness (~100 nm). For the two different polymers, a peak corresponding to the structural relaxation process (α-process), the dielectric signature of the dynamic glass transition, is present. Compared to neat PS, the dielectric loss of *l*-PS increased by a factor of ~15 (for thick films). Analysis of the segmental mobility provided that the labeling with DR1 probe molecules of 1.25% of the aromatic rings does not alter the glass transition temperature (= 100.3 ± 1.0 °C) or the dynamic fragility m (= 131 ± 10), i.e., the steepness of the temperature dependence of the structural relaxation, of polystyrene. A complete relaxation map of the two polymers is provided in the Supporting Information.

Reduction of the thickness strongly affected the gain in the dielectric strength. Figure 1a shows the isochronal representation of the dielectric loss at 1 kHz for films of various thicknesses, ranging from 10 to 106 nm, revealing a systematic decrease of the intensity of the α-peak. For comparison, the dielectric loss of single layers of neat PS is reported in Figure 1b. It is noteworthy that for the neat polymer the α-peak does not show any significant alteration down to a thickness of 25 nm, even after severe annealing (see Supporting Information). In addition to the reduction of $\Delta\varepsilon$, two other main features characterizing the thickness dependence on the α-process of several other polymers are present for *l*-PS. Upon reduction of the thickness, the maximum of the α-peak (T_α) shifts (here toward higher temperatures, which is indicative for a slowing down of the molecular dynamics), while the width of the α-peak increases due to a broadening of the distribution of the dynamic glass transition process.

On the basis of these findings, we reasoned that the different behavior between the neat PS and *l*-PS arises from a specific interaction of the chromophore with the substrate. We can argue that due to the presence of polar groups in the dye moiety (DR1) the *l*-PS can establish a large number of contact points (forming H-bonds) with the OH sites of the Al surface.

In an attempt to explore this hypothesis and to determine the actual depth profile of the glass transition dynamics, we prepared multilayer films of *l*-PS and neat PS, placing the chains with higher dielectric signal at specific positions inside films of neat PS. Regardless of the reduction of $\Delta\varepsilon$, even at 15 nm, the *l*-PS is well-suited for this study because of a sufficient contrast in dielectric signal over neat PS.

Values of the glass transition temperature measured in different geometries are plotted as a function of the film thickness in Figure 2 (geometry 1). A continuous increase of T_g up to 4 °C at 19 nm is observed for single layers of *l*-PS. The increase of T_g upon thickness reduction can be explained in terms of a reduction of mobility in proximity of the metallic interface, as already discussed in previous work.[18,39] Because of strong favorable polymer−substrate interactions, polymer chains in intimate contact with the solid interface are partially absorbed and consequently exhibit a slower dynamics compared to their behavior in bulk.[40] The resulting perturbations in the dynamics and structure (local packing) propagate into the depth of the film and decay after a characteristic distance, rationalized by a reduced mobility layer (RML) after which bulk mobility is largely recovered.[18] The RML would correspond to a layer of chains physisorbed at the interface where a certain fraction of its monomers is bound onto the surface and have almost zero mobility. The extension of the RML depends on various parameters such as the substrate polymer interaction and on the flexibility of the polymer chains. At higher surface to volume ratios (reduction of the thickness), due to the reduction of the bulk component, interfacial layers have a larger impact on the film properties.

Under those conditions, we can rationalize the tremendous drop by merely 85% of $\Delta\varepsilon$ compared to the bulk value observed for the thinnest samples (see Figure 2 (geometry 1)). A reduction of the dielectric strength corresponds, in fact, to a decrease of the density of the fluctuating dipoles, contributing to the dielectric signal. In amorphous ultrathin polymer films, this trend can be explained by considering that due to the reduced mobility, interfacial chains have a lower or almost zero value of $\Delta\varepsilon$. For *l*-PS the reduction of $\Delta\varepsilon$ scales with the inverse of the thickness, in line with data reported for other polymers.[41−43] This trend corresponds to a profile of molecular mobility sketched by the steplike function as in the inset of Figure 2b, related to a bilayer model system where a bulklike core is sandwiched between two dead layers (DL), i.e., a fraction of molecules where the structural relaxation is inhibited over the whole experimental temperature range. The dimension of the DL was estimated extrapolating to the thickness where the condition $\Delta\varepsilon$ = 0 is achieved. From our results we evaluated a $DL_{PS\text{-}DR1} \sim 6$ nm, a value larger than the one reported for a strongly adsorbing polymer like poly(2-vinylpyridine) on Al (~3 nm)[44] and in agreement with the one extrapolated for a low molecular weight *l*-PS on Al (~7 nm).[37]

3.2. Impact of Annealing on the Distributions of T_g and Dielectric Strength. To investigate the influence of annealing on the behavior of chains at the interface, we measured the response of multilayer films both during heating (RT → 150 °C) and cooling (150 °C → RT) scans (effective scanning rate 0.3 °C/min), a condition which corresponds to respectively short and long annealing times. In fact, changes in the properties of ultrathin films held above T_g scale with the same activation energy as the structural relaxation; i.e., annealing

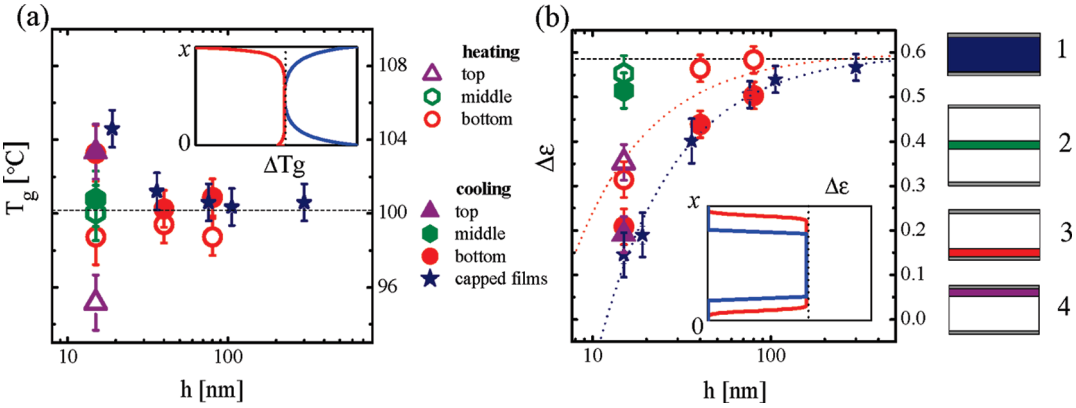

Figure 2. Values of glass transition temperature, T_g (a), and dielectric strength, $\Delta\varepsilon$ (b), are reported for different thickness and sample configurations. Colors of the symbols correspond to the color chosen for the different geometries sketched on the right. Open symbols are used for the values measured in heating and solid symbols for those in cooling. Sketches of the profiles of T_g (a) and $\Delta\varepsilon$ (b) along the film thickness in heating (red) and in cooling (blue) are given as insets.

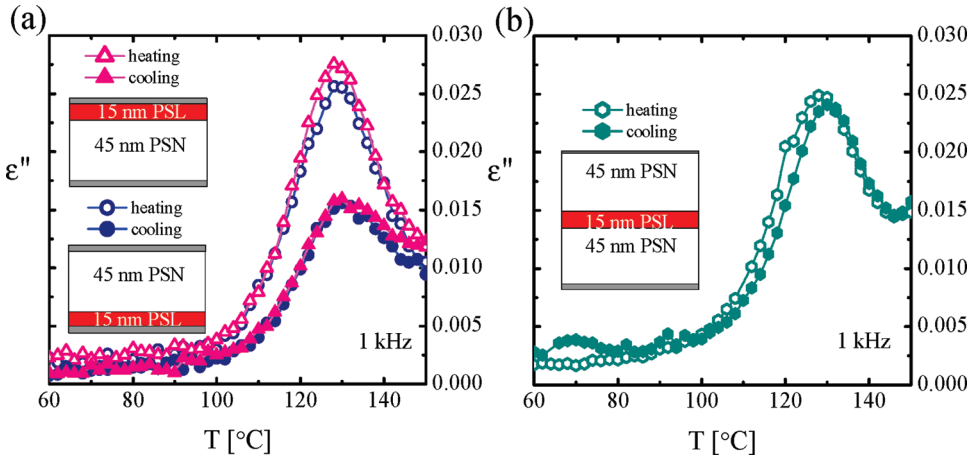

Figure 3. Temperature dependence of the imaginary part of the total dielectric function at 1 kHz in heating (open symbol) and cooling scans (full symbol) for (a) bilayer films in geometries 3 and 4 and (b) trilayer film in geometry 2.

at higher temperatures compares to longer annealing times at a lower temperature, provided that time−temperature superposition is fulfilled.

We first analyzed the total dielectric signal of multilayer films obtained by assembling layers of 45 nm thick layers of PS neat and 15 nm thick layers of labeled PS (see Figure 3). Comparing the signal in heating and cooling, we observed a reduction of the peak height as the result of annealing only when the *l*-PS layer was in direct contact with the metal. On the contrary, no relevant changes of the dielectric loss curve have been found for the trilayer film, where the labeled layer was placed between two thick layers of neat PS. These findings clearly support our picture that this reduction of $\Delta\varepsilon$ originates from a specific interaction between the polymer and the substrate, which, in this specific case, is physisorption of dye moieties at the metallic interface. This is further in line with the idea that deviations from bulk behavior originates from conformations assumed by the absorbed chains at the interfaces.[44]

Extracting the response of the labeled layer from the total dielectric function of the multilayer film, we were able to quantify the segmental dynamics and the dielectric strength at different distances from the interface and check their evolutions upon annealing. Such a procedure is facilitated by the difference in dielectric strength between the two different layers and justified by our previous work on averaging of the dielectric signal in ultrathin polymer films.[18,24] In particular, considering the identical values of T_g and the same fragility values, the dynamics of the doped polymer in contact with neat PS corresponds to the dynamics of *l*-PS enslaved to its own gradient of mobility.[26,27] A 15 nm thick layer of *l*-PS placed in between two 45 nm layers of neat PS (geometry 2) exhibits a bulk T_g over the two thermal cycles of heating and cooling, and its $\Delta\varepsilon$ does not show any reduction either compared to the bulk value or as a consequence of the annealing.[45] On the contrary, the dielectric strength of layers of labeled polymer of the same thickness placed in direct contact with the metallic interfaces (geometries 3 and 4) was reduced by roughly one-third already during the heating scan. After reaching 150 °C and successive cooling, $\Delta\varepsilon$ dropped further until reaching ~30% of its bulk value. It is worth reminding that the sample preparation of the layers in the two geometries is rather different. Soon after assembling of the multilayers, the conformations adopted by polymer chains in geometries 3 and 4 are intrinsically dissimilar: at the lower interface (geometry 3) chains adsorption starts already during spin-coating of dilute solutions on the metal, while at the upper electrode (geometry 4), molecules facing a free surface are finally covered by metal atoms thermally evaporated in high vacuum. The asymmetry in the sample preparation is probably erased within the times scale of the structural relaxation time, i.e., considering our slow scanning rates (~0.5 °C/min) differences between the two interfaces disappear soon after holding the multilayers above T_g.

The segmental dynamics showed a dependence on the thermal cycles implying a metastable character of the chain conformations. One of the criteria to identify thermodynamic equilibrium is in fact stability against annealing.[46] In particular, the layer placed in the top position of the film (geometry 4) displayed an enhancement of T_g compared to the bulk during the heating scan (short annealing) and an increased T_g upon cooling (long annealing).

Similar results were found for films of neat PS of lower molecular weight (M_w = 160 kg/mol)[47] where it was possible to tune T_g within 45 °C by simply varying the annealing conditions.[39] Samples annealed at 100 °C for 12 h exhibited a glass transition temperature lower than in bulk and could be schemed as trilayers composed by a dead layer in contact with the lower electrode, a free surface stacked underneath the upper electrode and a bulklike layer embedded in between. On the contrary, an increase of T_g was measured for films annealed for the same time at 120 °C, and analysis of the thermal expansivity proved that the free surface was transformed into a dead layer. In this experiment, it was not possible to discriminate between an enhancement of molecular mobility due to the presence of a free surface and an overall reduction of the segmental mobility imputable to the presence of residual solvent. The multilayer approach allowed us to disentangle these two effects.

An enhancement of segmental mobility coupled to a reduction of $\Delta\varepsilon$ due to adsorption of polymer chains at the interface may, however, appear contradictory. Nevertheless, the behavior we found for interfacial chains during heating scans is in line with a recent study on the confinement effects on thermal expansivity and T_g of ultrathin films of poly(*tert*-butylstyrene) capped between aluminum layers.[20] The nonintuitive decrease of T_g appearing simultaneously with a reduction of the thermal expansivity was explained in terms of a conformation−density coupling of rigid chains at the interface. Polymer segments at the very interface are anchored to the metal surface and form a dead layer with a reduced thermal expansivity. At longer distances from the substrate the presence of a bulky group in the PTBS chains reduces the packing efficiency of the polymer segments and thus leads to an increase of free volume and a corresponding reduction of T_g.[48] The same arguments can be taken in consideration to explain how 15 nm thick layers of labeled PS at the interface can mimic the behavior of a free surface with a reduced T_g (in the heating ramp) even if the polymer segments are already adsorbed.

Because of a longer annealing (cooling ramp), at the upper interface the T_g increased up to 8 °C and the dielectric strength was further reduced (see Figure 2), reaching the same values of the lower interface. These findings can be readily interpreted in terms of a growth and evolution of the adsorbed polymer layer at the interface. Annealing would lead to a state where the initially adsorbed polymer chains endure internal relaxation processes and become progressively more attached to the surface.[49] This process needs rearrangement and deformation of already adsorbed chain segments and brings to a larger surface coverage or higher concentration of the adsorbed layer. The resulting improved packing causes a reduction of the free volume and a consequent increase of T_g.

This hypothesis is confirmed by the impact of interfaces on the distribution of relaxation times, $L(\tau)$[50] (see Figure 4). By means of the HN parameters obtained by fitting isothermal spectra via eq 1, we calculated the distribution relaxation times for a 106 nm thick film of labeled PS in the capped configuration (geometry 1) and for a 15 nm thick layer of the same polymer placed in the upper position (geometry 4).

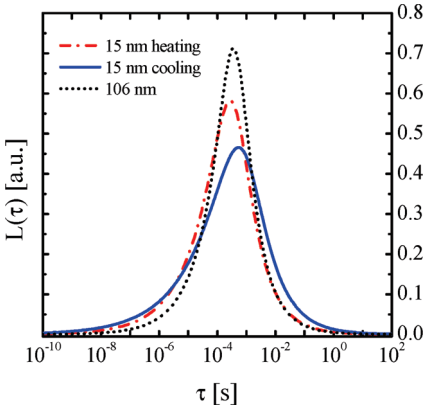

Figure 4. Distribution relaxation times $L(\tau)$ of the α-process at 130 °C for layers of labeled PS for a thick sample (106 nm) in geometry 1 (dot) and a 15 nm thick layer in geometry 3 during heating (dash dot) and cooling (solid).

Compared to the thicker film, the peak maximum of the interfacial layer is shifted toward shorter times in heating and longer times in cooling following the trend observed for the glass transition temperature. In the proximity of the attractive interface, $L(\tau)$ broadens manifesting a more heterogeneous character of the relaxation mechanism, in line with the broadening observed for the α-peak of ultrathin polymer films. At the upper interface, the distribution of relaxation times of layers heated from RT to 130 °C shows an enrichment toward short time scales, confirming the faster dynamics mimicking the free surface effect. More rigorous annealing (130 °C → 150 °C → 130 °C) leads to a further broadening of the peak due to the appearance of slower relaxation modes, related to the reduced mobility in the mature adsorbed layers. These findings support the physical pictures described above.

Thicker layer of *l*-PS placed at the bottom of the film (40 and 80 nm in geometry 3, Figure 2) did not show any deviation from the bulk behavior, suggesting that the perturbations on the mobility and the chains conformation decay at a few tens of nanometers from the bounding interface. The drop of $\Delta\varepsilon$ in the physisorbed layer, however, reduces the weight of those interfacial chains, assuming conformations different from the bulk and generating the perturbation in T_g. As a consequence, the profile in molecular mobility might appear sharper than in the case of those obtained by measuring quantities constant all over the film thickness.

4. Conclusions

We have developed a multilayer approach by exploiting the advantages of dielectric relaxation spectroscopy that allowed us to access the actual depth profile of the cooperative segmental mobility in ultrathin polymer films capped between aluminum layers. Selectively placing layers of dye-labeled PS at different distances from the metallic interfaces, we have been able to map the values of the glass transition temperature and the dielectric strength inside the film. We observed local changes in T_g and $\Delta\varepsilon$ exclusively when the labeled polymer was in direct contact with the Al surface. Polymer properties recovered bulk values at a distance from each interface smaller than 45 nm. On the other hand, in the proximity of bounding interfaces we observed a drop in $\Delta\varepsilon$ (chain pinning) already at short annealing times in conjunction with an unexpected reduction of T_g (packing frustration), which cannot be explained in terms of the effect of a free surface. A further decrease of $\Delta\varepsilon$ upon annealing was finally accompanied by an increase of T_g. We explained these experimental findings considering the evolution of an "imperfect" adsorbed layer,

characteristic of short annealing times into more mature physisorbed chains where an improvement of chains packing inhibits chain mobility and consequently increases T_g.

Universal features observed for the dielectric behavior of ultrathin films, i.e., reduction of the dielectric strength, broadening of the α-peak, and shift of the structural relaxation time, are finally rationalized by the physical picture here proposed. Out of our experimental results, we conclude that chain organization and its evolution upon annealing are key parameters in rationalizing the thermal properties of polymer layers at interfaces and should be included in future models on the deviation on bulk behavior.

Acknowledgment. C.R. acknowledges financial support from the Research Council of the K.U. Leuven, project no. OT/30/06. S.N. acknowledges FWO (Fonds Wetenschappelijk Onderzoeks - Vlaanderen) for a postdoctoral scholarship.

Supporting Information Available: Relaxation map and impact of annealing on the dielectric strength of labeled and neat polystyrene of high molecular weight; synthetical schemes and characterization of the chromophore/functionalized polystyrene. This material is available free of charge via the Internet at http://pubs.acs.org.

References and Notes

(1) Opila, R. L.; Eng, J. *Prog. Surf. Sci.* **2002**, *69*, 125−163.
(2) Shin, K.; Obukhov, S.; Chen, J. T.; Huh, J.; Hwang, Y.; Mok, S.; Dobriyal, P.; Thiyagarajan, P.; Russell, T. P. *Nature Mater.* **2007**, *6*, 961–965.
(3) O'Connell, P. A.; McKenna, G. B. *Science* **2005**, *310*, 1431–1431.
(4) Capitan, M. J.; Rueda, D. R.; Ezquerra, T. A. *Macromolecules* **2004**, *37*, 5653–5659.
(5) Napolitano, S.; Wübbenhorst, M. *Macromolecules* **2006**, *39*, 5967–5970.
(6) Martin, J.; Mijangos, C.; Sanz, A.; Ezquerra, T. A.; Nogales, A. *Macromolecules* **2009**, *42*, 5395–5401.
(7) Bertoldo, M.; Labardi, M.; Rotella, C.; Capaccioli, S. *Polymer* **2010**, *51*, 3660−3688.
(8) Zheng, X.; Rafailovich, M. H.; Sokolov, J.; Strzhemechny, Y.; Schwarz, S. A.; Sauer, B. B.; Rubinstein, M. *Phys. Rev. Lett.* **1997**, *79*, 241–244.
(9) Frank, B.; Gast, A. P.; Russell, T. P.; Brown, H. R.; Hawker, C. *Macromolecules* **1996**, *29*, 6531–6534.
(10) Forrest, J. A.; DalnokiVeress, K.; Dutcher, J. R. *Phys. Rev. E* **1997**, *56*, 5705–5716.
(11) Schönhals, A.; Goering, H.; Schick, C. *J. Non-Cryst. Solids* **2002**, *305*, 140–149.
(12) Kawana, S.; Jones, R. A. L. *Phys. Rev. E* **2001**, 63, no. *021501*.
(13) Forrest, J. A.; Dalnoki-Veress, K.; Stevens, J. R.; Dutcher, J. R. *Phys. Rev. Lett.* **1996**, *77*, 2002–2005.
(14) DeMaggio, G. B.; Frieze, W. E.; Gidley, D. W.; Zhu, M.; Hristov, H. A.; Yee, A. F. *Phys. Rev. Lett.* **1997**, *78*, 1524–1527.
(15) Tate, R. S.; Fryer, D. S.; Pasqualini, S.; Montague, M. F.; de Pablo, J. J.; Nealey, P. F. *J. Chem. Phys.* **2001**, *115*, 9982–9990.
(16) Keddie, J. L.; Jones, R. A. L.; Cory, R. A. *Faraday Discuss.* **1994**, 219–230.
(17) Fragiadakis, D.; Pissis, P. *J. Non-Cryst. Solids* **2007**, *353*, 4344–4352.
(18) Napolitano, S.; Prevosto, D.; Lucchesi, M.; Pingue, P.; D'Acunto, M.; Rolla, P. *Langmuir* **2007**, *23*, 2103–2109.
(19) Gun'ko, V. M.; Borysenko, M. V.; Pissis, P.; Spanoudaki, A.; Shinyashiki, N.; Sulim, I. Y.; Kulik, T. V.; Palyanytsya, B. B. *Appl. Surf. Sci.* **2007**, *253*, 7143–7156.
(20) Napolitano, S.; Pilleri, A.; Rolla, P.; Wübbenhorst, M. *ACS Nano* **2010**, *4*, 841−848.
(21) de Gennes, P. G. *Eur. Phys. J. E* **2000**, *2*, 201–203.
(22) Lipson, J. E. G.; Milner, S. T. *Eur. Phys. J. B* **2009**, *72*, 133–137.
(23) Peter, S.; Meyer, H.; Baschnagel, J. *J. Polym. Sci., Part B: Polym. Phys.* **2006**, *44*, 2951–2967.
(24) Peter, S.; Napolitano, S.; Meyer, H.; Wübbenhorst, M.; Baschnagel, J. *Macromolecules* **2008**, *41*, 7729−7743.
(25) Priestley, R. D.; Ellison, C. J.; Broadbelt, L. J.; Torkelson, J. M. *Science* **2005**, *309*, 456–459.
(26) Ellison, C. J.; Torkelson, J. M. *Nature Mater.* **2003**, *2*, 695–700.
(27) Roth, C. B.; Torkelson, J. M. *Macromolecules* **2007**, *40*, 3328–3336.
(28) Roth, C. B.; McNerny, K. L.; Jager, W. F.; Torkelson, J. M. *Macromolecules* **2007**, *40*, 2568–2574.
(29) Koeckelberghs, G.; Sioncke, S.; Verbiest, T.; Persoons, A.; Samyn, C. *Polymer* **2003**, *44*, 3785–3794.
(30) Reiter, G.; Hamieh, M.; Damman, P.; Sclavons, S.; Gabriele, S.; Vilmin, T.; Raphael, E. *Nature Mater.* **2005**, *4*, 754–758.
(31) Whitlow, S. J.; Wool, R. P. *Macromolecules* **1991**, *24*, 5926–5938.
(32) Wübbenhorst, M.; van Turnhout, J. *J. Non-Cryst. Solids* **2002**, *305*, 40–49.
(33) Havrilia., S.; Negami, S. *Polymer* **1967**, *8*, 161–&.
(34) Vogel, H. *Z. Phys.* **1921**, *22*, 645.
(35) van den Berg, O.; Sengers, W. G. F.; Jager, W. F.; Picken, S. J.; Wübbenhorst, M. *Macromolecules* **2004**, *37*, 2460–2470.
(36) Rotella, C.; Napolitano, S.; Wuebbenhorst, M. *Macromolecules* **2009**, *42*, 1415–1417.
(37) Priestley, R. D.; Broadbelt, L. J.; Torkelson, J. M.; Fukao, K. *Phys. Rev. E* **2007**, 75.
(38) van den Berg, O.; Wübbenhorst, M.; Picken, S. J.; Jager, W. F. *J. Non-Cryst. Solids* **2005**, *351*, 2694–2702.
(39) Napolitano, S.; Wübbenhorst, M. *J. Phys. Chem. B* **2007**, *111*, 9197–9199.
(40) vanZanten, J. H.; Wallace, W. E.; Wu, W. L. *Phys. Rev. E* **1996**, *53*, R2053–R2056.
(41) Labahn, D.; Mix, R.; Schonhals, A. *Phys. Rev. E* **2009**, *79*, 9.
(42) Fukao, K.; Uno, S.; Miyamoto, Y.; Hoshino, A.; Miyaji, H. *Phys. Rev. E* **2001**, 6405.
(43) Serghei, A.; Tress, M.; Kremer, F. *Macromolecules* **2006**, *39*, 9385–9387.
(44) Napolitano, S.; Lupascu, V.; Wübbenhorst, M. *Macromolecules* **2008**, *41*, 1061–1063.
(45) The experimental evidence that both the dielectric strength and the glass transition temperature of a layer of *l*-PS placed in between layers of neat PS are not altered compared to their bulk values further proves the validity of our subtraction procedure.
(46) Reiter, G.; Napolitano, S. *J. Polym. Sci., Part B: Polym. Phys.*, in press (DOI: 10.1002/polb.22134).
(47) Owing to diffusion coefficients 3 orders of magnitudes smaller, the kinetics of adsorption of this lower M_w is expected to be several orders of magnitude faster than the one used in this work.
(48) Ellison, C. J.; Mundra, M. K.; Torkelson, J. M. *Macromolecules* **2005**, *38*, 1767–1778.
(49) Schneider, H. M.; Frantz, P.; Granick, S. *Langmuir* **1996**, *12*, 994–996.
(50) Runt, J.; Fitzgerald, J. J. *Dielectric Spectroscopy of Polymeric Materials: Fundamental and Applications*; American Chemical Society: Washington, DC, 1997.